



**Full Length Article**

# Detection of Aflatoxin-Contaminated Cocoa Beans through YOLO Algorithm and Fluorescence Imaging

Muhammad Syukri Sadimantara<sup>1,2\*</sup>, Bambang Dwi Argo<sup>3†</sup>, Sucipto Sucipto<sup>1†</sup>, Dimas Firmanda Al Riza<sup>3†</sup> and Yusuf Hendrawan<sup>3†</sup>

<sup>1</sup>Department of Agroindustrial Technology, Universitas Brawijaya, Malang, 65145, Indonesia

<sup>2</sup>Department of Food Science and Technology, Universitas Halu Oleo, Kendari, 93231, Indonesia

<sup>3</sup>Department of Biosystems Engineering, Universitas Brawijaya, Malang, 65145, Indonesia

\*For correspondence: [syukrisadimantara@uho.ac.id](mailto:syukrisadimantara@uho.ac.id)

†Contributed equally to this work

Received 24 August 2023; Accepted 22 September 2023; Published 05 October 2023

## Abstract

This research aimed to develop detection model for aflatoxin-contaminated cocoa beans using YOLO (You Only Look Once) method based on fluorescence imaging. Aflatoxin level measurement and image acquisition were carried out on cocoa beans inoculated with *Aspergillus flavus* (6 mL/100 g) and incubated for 7 days. The quantification of aflatoxin levels was achieved through Liquid Mass Chromatography (LCMS), which served as the basis for categorizing the images into 3 groups, namely aflatoxin-free, contaminated below and contaminated above the threshold. The image acquisition was conducted in a mini studio equipped with UV light. Furthermore, image annotation was carried out using Roboflow, while YOLOv5 was employed as detection model for aflatoxin-contaminated cocoa beans. The performance of YOLO model, based on testing data, yielded the following metrics: precision (all): 0.91, recall (all): 0.93, mean average precision (all): 0.95 and mAP@[.5:.95] (all): 0.47. The average accuracy based on the confusion matrix from the testing data was 91%. These results showed that a combination of YOLOv5 model and fluorescence imaging presented a highly performing alternative for detecting various aflatoxin contamination levels in cocoa beans. © 2023 Friends Science Publishers

**Keywords:** Aflatoxin; Cocoa beans; Object detection; Fluorescence imaging; YOLO

## Introduction

Aflatoxin is currently a global food safety concern, affecting sensory quality, causing trade loss (Wu 2015) and posing health risks such as cancer, mutations, immunosuppression, renal toxicity, and more (Rushing and Selim 2019). Among the various model responsible for aflatoxin production, *Aspergillus flavus* and *Aspergillus parasiticus* are the most common and toxic types (Wu *et al.* 2021). Aflatoxin is a secondary metabolite generated by *A. flavus*, affecting various agricultural commodities including peanuts (Osaili *et al.* 2023), corn (Cabrera-Meraz *et al.* 2021), rice (Dachoupan Sirisomboon *et al.* 2013) and cocoa beans (Oliveira *et al.* 2009). Cocoa is an internationally valued commodity, with the export value and products reaching \$50.09 in 2018-2019 (Voora *et al.* 2019). However, inadequate cocoa beans handling can facilitate the growth of *A. flavus* (Copetti *et al.* 2014), necessitating early detection before entering cocoa supply chain, as it remains stable under storage, processing, and production conditions. Cocoa beans are also subject to stringent trading requirements, including

international authorities such as the European Commission limiting the intake of total aflatoxin to 20 ppb (European Commission 2014).

Computer vision has been applied in detecting aflatoxin contamination in various agricultural products as an alternative to chemical methods such as Enzyme-Linked Immunosorbent Assay (ELISA) and Polymerase Chain Reaction (PCR) methods. Although these methods accurately quantify mycotoxin contamination, the drawbacks include high costs, time consumption, destructiveness and requiring expertise from laboratory personnel (Hassoun and Romdhane 2015). Among the computer vision methods for mycotoxin detection are Color Imaging (Polisenska 2011), Near-infrared (NIR) Spectroscopy (Mallmann *et al.* 2020), Mid-infrared (MIR) Spectroscopy (Kaya-celiker *et al.* 2015), NIR Hyperspectral Imaging (Thiruppathi 2016) and X-Ray Imaging (Du *et al.* 2019). Each of these technologies has its advantages and disadvantages, with Color Imaging exhibiting high detection accuracy of up to 89% but having a limited electromagnetic range, preventing early mycotoxin contamination detection (Tallada *et al.* 2011).

Ultraviolet (UV)-Induced fluorescence imaging can be an alternative in aflatoxin detection by using the excitation-emission properties of fluorescence light, where each organic material, including aflatoxin, possesses distinct fluorescence characteristics (Cozzini *et al.* 2008). Aflatoxin has excitation and emission wavelengths of 365 nm and 455 nm, respectively (Kamilaris and Prenafeta-Boldú 2018). Several investigations have been carried out on exploiting fluorescence properties, including Hyperspectral fluorescence imaging for detecting aflatoxin in corn (Hruska *et al.* 2017). However, the hyperspectral method requires relatively expensive equipment, indicating the need for simpler technology. Rotich *et al.* (2020) 365 nm LEDs were used in a color camera as the excitation light source to record the optical properties of fluorescence images created by UV light in the visible area. The target fluorophores were found to be able to emit in the visible area, allowing for the employment of simplified imaging techniques.

The rapid development of deep learning algorithms in object detection has been remarkable, including YOLO which is categorized as a one-stage algorithm (Wang and Yan 2021). This algorithm exhibits superior detection speed compared to two-stage algorithms such as R-CNN, Fast R-CNN and Faster R-CNN (Sanchez *et al.* 2020). YOLOv5 represents the fifth generation of YOLO algorithm, written in the Python programming language (Thuan 2021) and is a popular series due to its high accuracy and inference speed (Arifando *et al.* 2023). In this research, YOLOv5 was employed due to its advantages over other versions, including the newer YOLOv7. According to Olorunshola *et al.* (2023), YOLOv5 outperformed YOLOv7 in terms of speed and accuracy, which had been applied to agricultural product quality detection with high-performance models shown in research focusing on detecting fruits such as lychee (Wang *et al.* 2022) and tomatoes (Phan *et al.* 2023).

Based on the explanations above, this research aimed to detect cocoa beans at different aflatoxin contamination levels, namely aflatoxin-free, contaminated below and above the threshold. This was achieved through the quantification by LC-MS, using the UV-induced fluorescence imaging system for image acquisition, and employing YOLO algorithm for aflatoxin-contaminated cocoa beans detection. This research was carried out to offer an alternative for aflatoxin contamination detection in cocoa beans, exhibiting higher accuracy compared to other methods.

## Materials and Methods

### Experimental details and treatments

**Experimental materials:** The materials used in this research included the pure strain of *A. flavus* (Inacc F44) sourced from the Microbiology Laboratory collection at the Indonesian Institute of Sciences (LIPI) Cibinong. The forastero-type cocoa beans were obtained from the Indonesian Coffee and Cocoa Research Institute (Puslitkoka) with characteristics of

fermented beans, 6% moisture content, free from mycotoxin contamination and intact. Chemical substances employed encompass potato dextrose broth (PDB), distilled water, NaCl, alcohol and methanol.

**Treatments:** For fungus inoculum, the pure culture of *A. flavus* was cultivated in 10 mL liquid nutrient broth (NB) to obtain fungal inoculum, which was incubated for 3 days at room temperature. The resuspended culture was reinoculated in 100 mL of NB medium and incubated for 3 days at room temperature. The resulting culture was further inoculated in 1000 mL of NB medium and incubated for 3 more days at room temperature to obtain the inoculum stock for cocoa beans inoculation. Subsequently, the fungal inoculum was inoculated to cocoa beans at 60 mL/kg, incubated at 30°C and 90% RH in an incubator for 7 days after *A. flavus* inoculation.

### Measurement of aflatoxin levels

The aflatoxin levels in the samples were determined using LCMS. The LC system included an Agilent 1100MSD SL mass spectrometry detector with an orthogonal ESI nozzle, a Shimadzu pump model (Shimadzu, Kyoto, Japan), a fluorescence detector (RF- 10AXL), an auto-injector (SIL-10A), and a control system. The AF standard and pure samples were dissolved in 1 mL of mobile phase solution before being added to a 6  $\mu$ L LCMS/ESI. Protons, [M+ H]<sup>+</sup>, with a residence time of 1,000 ms per ion were found in all of the tested AFs. For LC analysis, the test tube holding the pure sample or the aflatoxin working standard was added with 0.1 mL of TFA. The selected ions (m/z) targets were measured at 313, 315, 329 and 331, respectively, were AFB<sub>1</sub> and AFG<sub>2</sub>. The tube was vortexed, diluted with 0.9 mL of an acetonitrile-water solution (1:9) and allowed to sit in the dark for 15 min at room temperature. The resulting solution was then tested for reverse phase LC analysis using 20  $\mu$ L. Using Electrospray Ionization (ESI) in Multiple Reaction Monitoring (MRM) modes, aflatoxin was discovered. The results of the LC/MS-MS data analysis gave the extracts compounds molecular weight and chromatogram in the form of peaks, allowing for the calculation of how many compounds were total in each sample. For each measurement, three times were performed.

### Image acquisition

A Canon L300 camera was used to capture images of cocoa beans for up to seven days following the inoculation of *A. flavus*. 400  $\times$  600-pixel JPG files were used to save the generated images. The image was captured in a studio that featured 365 nm UV LED lamp made by CCS Inc. in Japan. The UV lamp was positioned 350 mm away from the sample unit, emitting 6.9 Wm<sup>2</sup> of radiation on average. Additionally, a UV bandpass filter was placed in front of the UV light source and the camera to block out the light that was reflected. It performs similarly to a UV cut filter but only lets 0.3% of 365 nm to pass through. In the subunit of image

acquisition, a high-resolution CMOS camera of  $5 \times 3078$  pixels was used, namely the EOS Kiss  $\times 7$  (Canon Inc., Japan) with ISO 200, F-5.6 and manual exposure of 1/3 sec for fluorescence image recording placed 450 mm from the sample location. The image acquisition unit measures 18.5 cm  $\times$  18.5 cm  $\times$  29 cm and is connected to the light source through an optical fiber (Fig. 1).

### Detection modeling of aflatoxin-contaminated cocoa beans using YOLO

A total of 100 images were collected and the dataset was split into 70 training, 20 validation and 10 testing images. Image annotation was carried out using the Roboflow application on the 100 images, total of 1360 annotated object, specifically cocoa beans, with details of 470, 430 and 460 beans labeled as aflatoxin-free, below the threshold and above the threshold, respectively. Image pre-processing was performed through auto-orientation and resizing of images to  $640 \times 640$ . Image augmentation was applied to the training set to add data variation and enhance the performance of the network during training. Augmentation is carried out through horizontal flip and  $90^\circ$  clockwise rotate, a total of 210 augmented training images were obtained. Images dataset divided into 3 categories, including training (210 images / 88%), validation (20 images / 8%) and testing (10 images / 4%).

The model design consisted of 8 stages, namely 1) Importing libraries, 2) Importing the dataset, 3) Cloning YOLOv5 repository, 4) Installing YOLOv5 libraries, 5) Training YOLOv5 model with cocoa beans image dataset. Upon completion, the "YOLOv5\_training\_best\_weight" file containing the best network weights was generated. 6) Plotting metrics on Tensorboard, 7) Detecting aflatoxin-contaminated cocoa beans using the trained model on the test dataset and 8) Plotting images of detected aflatoxin-contaminated cocoa beans. YOLO algorithm settings for the experiment included batch size: 16, epochs: 200, initial learning rate: 0.01, deep learning library: PyTorch, weights: YOLOv5s.pt and optimization function: Adam, confidence threshold: 0.4 and IoU-threshold: 0.3 were set to test the output model.

### Performance of YOLOv5 model

The performance of YOLOv5 model was tested by calculating the confusion matrix, recall, precision and F1 score of the trained object detection networks (Yadav *et al.* 2022). Furthermore, a performance test was conducted on the 2 trained networks using 10 frames from the testing set.

### Results

The quantification test showed that aflatoxin was not detected within the RL =  $1 \mu\text{g}/\text{kg}$  limit in the control treatment. However, in the AF inoculation treatment from day 1 to day 7,

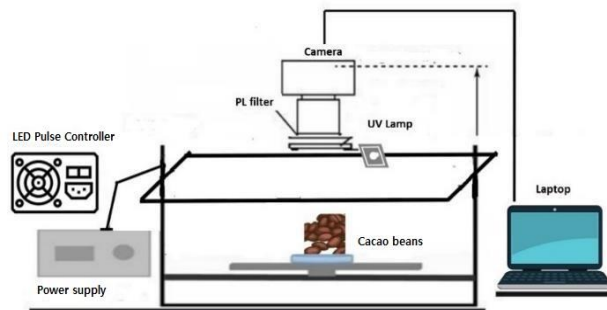


**Fig. 1:** Image acquisition unit

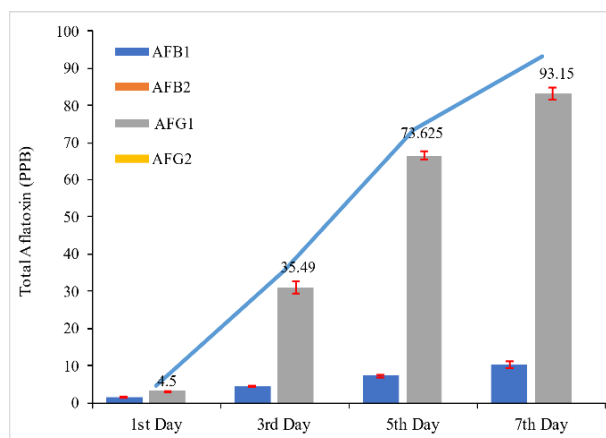


**Fig. 2:** Changes in aflatoxin levels after inoculation of *A. flavus* on cocoa beans

AFB<sub>2</sub> and AFG<sub>2</sub> were not detected. An increase in AFB<sub>1</sub> and AFG<sub>1</sub> levels was also observed in the *A. flavus* inoculation treatment. Among aflatoxin types, AFG<sub>1</sub> showed the highest increase, followed by AFB<sub>1</sub> at 83.10 ppb and 9.77 ppb on day 7, respectively (Fig. 2).

### Image analysis

Image labeling according to the level of aflatoxin contamination was carried out, namely on days 1–2 contaminated with aflatoxin below the threshold and days 3–7 contaminated with aflatoxin above the threshold (Fig. 3).

### Detection modeling of aflatoxin-contaminated cocoa beans

The acquired cocoa beans images were annotated using bounding boxes for 3 classes, namely aflatoxin-free, contaminated below the threshold and contaminated above the threshold, using the Roboflow application, as presented in (Fig. 4). The model was trained using the Google Colaboratory (Colab) cloud platform and a Notebook developed by Roboflow.ai based on YOLOv5. The model training with 200 epochs took approximately 5 min and a summary of YOLO model is given in Table 1.

**Table 1:** Training, validation, and testing performance of YOLOv5 model for aflatoxin contamination detection in cocoa beans

| Class | Training |      |      |                | Validation |      |      |               | Testing |      |      |               |
|-------|----------|------|------|----------------|------------|------|------|---------------|---------|------|------|---------------|
|       | P        | R    | mAP  | mAP@ [.5, .95] | P          | R    | mAP  | mAP@ [.5:.95] | P       | R    | mAP  | mAP@ [.5:.95] |
| All   | 0.99     | 0.99 | 0.99 | 0.51           | 0.89       | 0.93 | 0.95 | 0.52          | 0.91    | 0.93 | 0.95 | 0.47          |
| Free  | 0.99     | 0.99 | 0.99 | 0.46           | 0.86       | 0.92 | 0.94 | 0.47          | 0.88    | 0.89 | 0.91 | 0.44          |
| Above | 0.99     | 0.99 | 0.99 | 0.51           | 0.87       | 0.94 | 0.93 | 0.52          | 0.92    | 0.99 | 0.96 | 0.41          |
| Below | 0.99     | 1.00 | 0.99 | 0.56           | 0.95       | 0.93 | 0.93 | 0.57          | 0.91    | 0.95 | 0.98 | 0.57          |

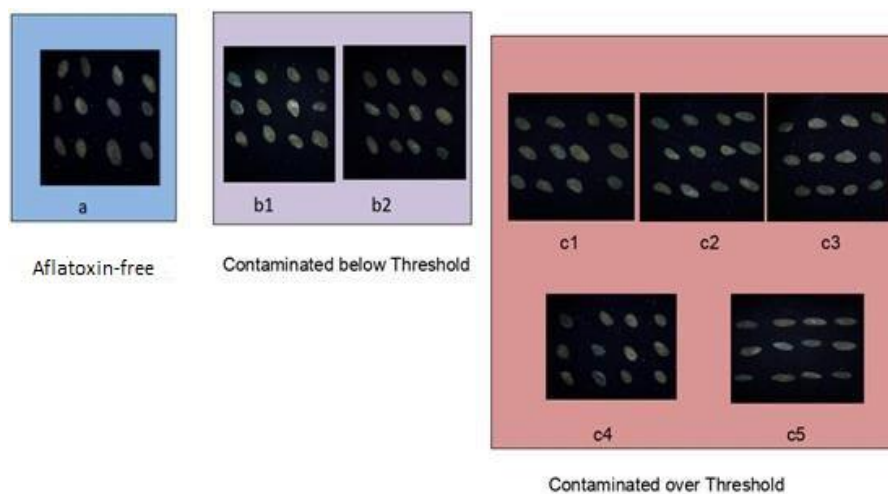


**Fig. 3:** Fluorescence images of cocoa beans as a result of *A. flavus* inoculation on days 1-7; a) control, (b1) day 1, (b2) day 2, (C1) day 3, (c2) day 4, (c3), day 5, (c4) day 6, (c5) day 7

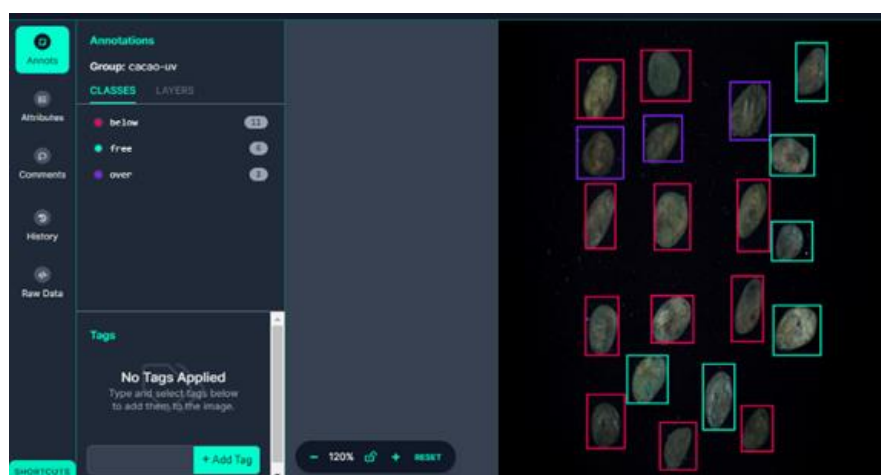


**Fig. 4:** An example of annotated fluorescence images with bounding boxes for detecting Afs-contaminated cocoa beans

Furthermore, the performance of YOLOv5 model on the testing data yielded precision (all): 0.91, recall (all): 0.93, mean average precision: 0.95, and mAP@[.5:.95]: 0.47. The improvement in the performance of YOLO model with each iteration as observed in (Fig. 5). showed different performance metrics for the training and validation sets. Other indicators such as precision-recall and F1-confidence curves were shown in (Fig. 6a,b).

The precision-recall curve summarized the tradeoff between the true positive rate and the predicted value for a prediction model using various probability thresholds. The

area under the curve was called average precision (AP), where a higher AP value or approaching 1 indicated a more reliable model for detecting target object. A larger area under the curve signified high recall and precision, relating to low false positive and recall rates. Based on the P-R curve, cocoa class “above the threshold” covered more area compared to the “below” and “free” classes, with a value of 0.976. The F1 score obtained for YOLO model was 0.91, indicating a high precision. The normalized confusion matrix of YOLO model on the testing data for detecting aflatoxin-contaminated cocoa beans was shown in (Fig. 7).

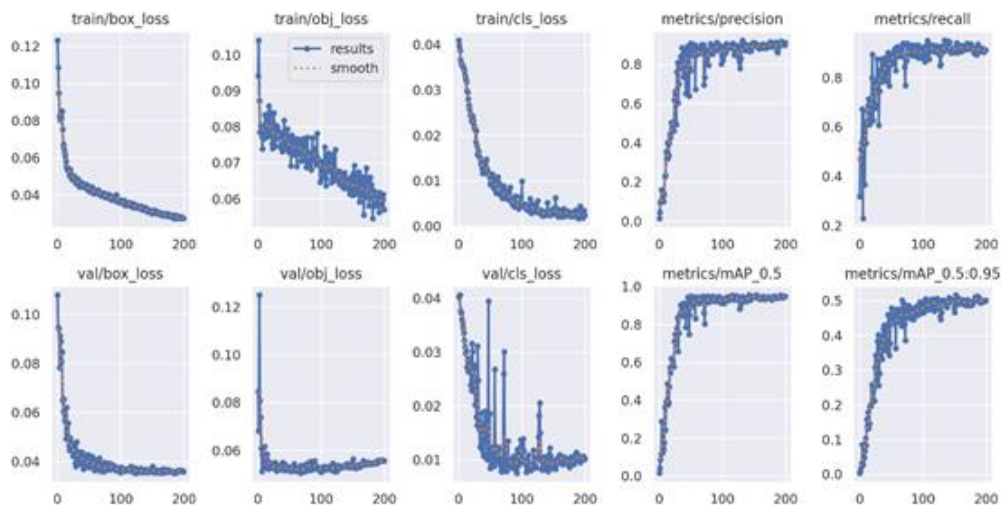


**Fig. 5:** Plots of box loss, objectness loss, classification loss, precision, recall, and mean average precision (mAP) through training epochs on training and validation sets

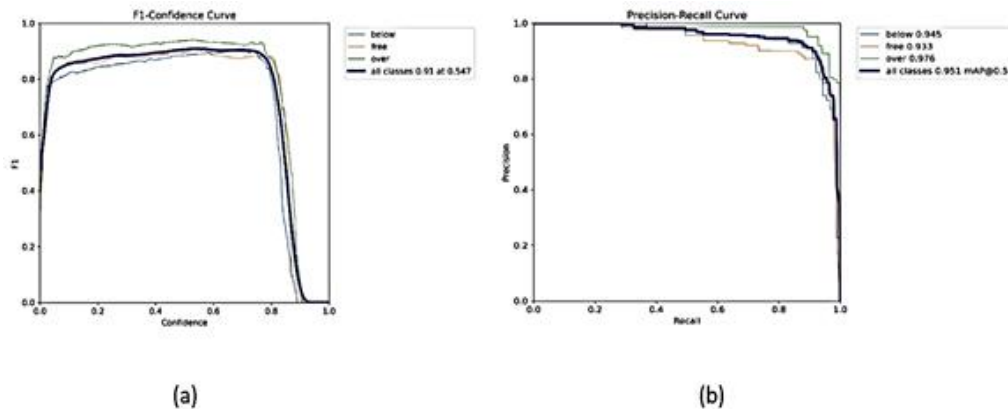


**Fig. 6:** YOLO model performance curves (a) F1 confidence (b) precision-recall

In Fig. 7, the Y-axis (True) represented the ground truth class of annotated cocoa beans images, while the X-axis (Predicted) indicated the predicted classes from the trained model. The values in each cell indicated the proportion of each true class that had been predicted for contamination levels. For instance, 90% of cocoa beans had been accurately detected as contaminated with aflatoxin below the threshold, while 10% were predicted as contaminated above the threshold. Based on the confusion matrix (Fig. 7), the model was capable of predicting cocoa beans at various aflatoxin contamination levels.

The output of YOLO model was represented by “best.pt” preserving the weights from the best epoch. The results included aflatoxin contamination detection equipped by bounding boxes with confidence scores, as shown in (Fig. 8). Where all cocoa beans in each contamination level were successfully detected. In terms of confidence scores in Fig. 8, there were cocoa beans with scores higher than 0.9, while some had 0.3.

## Discussion

Aflatoxin levels in cocoa beans in this research varied significantly in each observation. This aligned with Hruska *et al.* (2017), who examined aflatoxin measurements in maize kernels inoculated with *A. flavus*, and obtain a value exceeding the threshold by day 7. Based on the image acquisition results, cocoa beans images with blue UV light emission were observed on day 7. This emission occurred when fluorophores were excited by UV light at a specific wavelength, resulting in emission with a longer wavelength. AFB<sub>1</sub> and AFB<sub>2</sub> exhibited a blue fluorescence color, while AFG<sub>1</sub> and AFG<sub>2</sub> were green (Galaverna and Dall’Asta 2012).

The performance of aflatoxin contamination detection model in cocoa beans, with precision (all): 0.91, recall (all): 0.93, mean average precision (all): 0.95, and mAP@[.5:.95] (all): 0.47, showed that the model had performed well. Based on the object detection metric obtained, namely mAP, these results were better than the blueberry ripeness detection

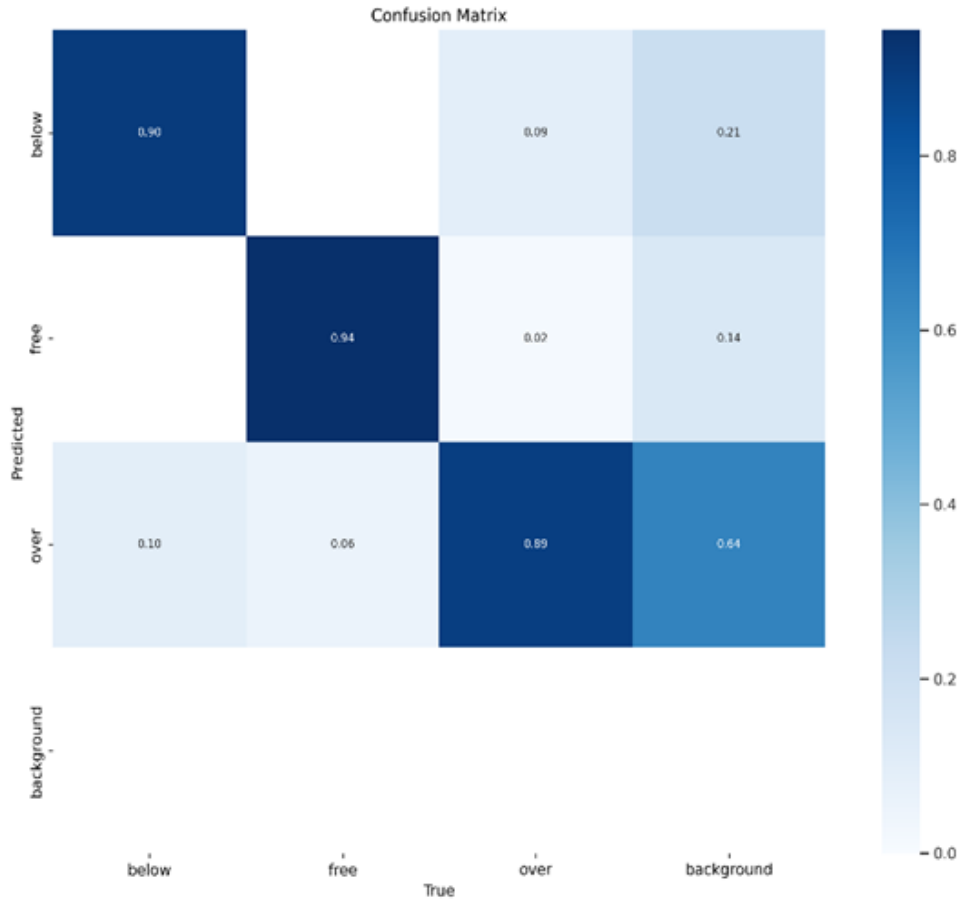


Fig. 7: Confusion matrix of YOLO model on testing data



Fig. 8: Images of testing dataset evaluated with YOLO model on fluorescence imaging

performance conducted by MacEachern *et al.* (2023), which achieved an mAP of 0.88. The higher the mAP value, the better the performance of the object detection algorithm. The results obtained are also not much different from the results from Jubayer *et al.* (2021) obtained precision, recall and average precision (AP) of 98.10, 100 and 99.60%, respectively, for mold detection on food surfaces.

The role of loss in the training process is crucial, as it reflects the relationship between true and predicted values. The smaller the loss value, the closer the predicted value is to a true value, resulting in better performance of the model. In this research, the three types of losses observed were noted namely box, objectness, and classification losses (Fig. 5). Box loss indicated how well the

algorithm precisely locate the center of object and the accuracy of the predicted bounding boxes to cover object. Minimum box loss showed the precision of bounding box positioning and enhanced estimation speed performance (Ye *et al.* 2023). Furthermore, objectness loss served as a measure of the probability that object existed in the proposed Region of Interest. A high objectness loss suggested that the image window might contain object (Hussain *et al.* 2021). Meanwhile, classification loss indicated how well the algorithm predicted the correct class of a given object (Kasper-Eulaers *et al.* 2021). Fig. 5 showed that the three losses for the training and validation sets exhibited decreasing trends and eventually stabilized. This suggested that the performance of the model rapidly improved in terms of precision, recall and mAP before reaching epoch 200. The validation data also showed rapid decreases up to around epoch 200, indicating the good object detection performance of the model.

The image test from the testing dataset evaluated with YOLO model on fluorescence images obtained varying confidence scores ranging from 0.3 to 0.9. This diverse accuracy occurred due to the presence of numerous objects in an image. According to Ma (2023), accuracy declined when multiple object were present in an image, such as in images of oranges with and without peel, exhibiting higher confidence scores that contained only 1 object.

## Conclusion

This research investigated the design of YOLO model based on fluorescence imaging with a wavelength of 365 nm for detecting aflatoxin-free cocoa beans, contaminated below the threshold, and above the threshold. The performance of the model on testing data yielded precision (all): 0.91, recall (all): 0.93, mean average precision (all): 0.95, and mAP@[.5:.95] (all): 0.47. Moreover, the average accuracy based on the confusion matrix for the testing data was 91%. These results showed that the combination of YOLOv5 model and fluorescence imaging could serve as a highly-performing alternative for detecting aflatoxin contamination levels in cocoa beans.

## Acknowledgements

The authors would like to acknowledge KEMENDIKBUD RISTEK, Lembaga Pengelola Dana Pendidikan (LPDP), and Beasiswa Pendidikan Indonesia (BPI) Indonesia for scholarship funding.

## Author Contributions

MSS conducting research and writing manuscript; BDA conducting research and review manuscript; SS conducting research and review manuscript; DFA conducting research and provide hardware; YH conducting research and review manuscript.

## Conflicts of Interests

All the authors declare that they have no competing interests.

## Data Availability

Data supporting the findings of this study are available from the corresponding author upon reasonable request.

## Ethics Approval

Not applicable to this paper.

## References

- Arifando R, S Eto, C Wada (2023). Improved YOLOv5-based lightweight object detection algorithm for people with visual impairment to detect buses. *Appl Sci* 13:5802
- Cabrera-Meraz J, L Maldonado, A Bianchini, R Espinal (2021). Incidence of aflatoxins and fumonisins in grain, masa and corn tortillas in four municipalities in the department of Lempira, Honduras. *Heliyon* 7:e08506
- Copetti MV, BT Imanaka, JI Pitt, MH Taniwaki (2014). Fungi and mycotoxins in cocoa: From farm to chocolate. *Intl J Food Microbiol* 178:13–20
- Cozzini P, G Ingleto, R Singh, C Dall'Asta (2008). Mycotoxin detection plays “cops and robbers”: Cyclodextrin chemosensors as specialized police. *Intl J Mol Sci* 9:2474–2494
- Dachoupan Sirisomboon C, R Putthang, P Sirisomboon (2013). Application of near infrared spectroscopy to detect aflatoxigenic fungal contamination in rice. *Food Contr* 33:207–214
- Du Z, N Ali, B Ashraf (2019). X-ray computed tomography for quality inspection of agricultural products: A review. *Food Sci Nutr* 7:3146–3160
- European Commission (2014). Commission implementing regulation (EU) No 884/2014 of 13 August 2014 imposing special conditions governing the import of certain feed and food from certain third countries due to contamination risk by aflatoxins and repealing regulation (EC) No 1152/2009. *Official J Eur Union* 2014:20–30
- Galaverna G, C Dall'Asta (2012). 4.16 – Sampling techniques for the determination of mycotoxins in food matrices. *Compr Sampl Sampl Prep* 4:381–403
- Hassoun A, K Romdhane (2015). Quality evaluation of fish and other seafood by traditional and nondestructive instrumental methods: Advantages and limitations. *Crit Rev Food Sci Nutr* 57:1976–1998
- Hruska Z, H Yao, R Kincaid, RL Brown, D Bhatnagar, TE Cleveland (2017). Temporal effects on internal fluorescence emissions associated with aflatoxin contamination from corn kernel cross-sections inoculated with toxigenic and atoxigenic *Aspergillus flavus*. *Front Microbiol* 8:1718
- Hussain A, B Barua, A Osman, R Abozariba, AT Asyhari (2021). Low latency and non-intrusive accurate object detection in forests. *IEEE Symp Ser Comput Intellig (SSCI)* 2021:1–6
- Jubayer F, JA Soeb, AN Mojumder, MK Paul, P Barua, S Kayshar, SS Akter, M Rahman, A Islam (2021). Detection of mold on the food surface using YOLOv5. *Curr Res Food Sci* 4:724–728
- Kamilaris A, FX Prenafeta-Boldú (2018). A review of the use of convolutional neural networks in agriculture. *J Agric Sci* 156:312–322
- Kasper-Eulaers M, N Hahn, PE Kummervold, S Berger, T Sebulonsen, Ø Myrland (2021). Detecting heavy goods vehicles in rest areas in winter conditions using YOLOv5. *Algorithms* 14:114
- Kaya-celiker H, PK Mallikarjunan, A Kaaya (2015). Mid-infrared spectroscopy for discrimination and classification of *Aspergillus* spp. contamination in peanuts. *Food Contr* 52:103–111
- Ma Y (2023). Automatic detection of oranges peel based on the YOLOv5 Model. *Highlights Sci Eng Technol* 34:176–182

- MacEachern CB, TJ Esau, AW Schumann, PJ Hennessy, QU Zaman (2023). Detection of fruit maturity stage and yield estimation in wild blueberry using deep learning convolutional neural networks. *Smart Agric Technol* 3:100099
- Mallmann CA, AO Mallmann, D Tyska (2020). Survey of mycotoxin in Brazilian corn by NIR spectroscopy. *Glob J Nutr Food Sci* 3:1–7
- Oliveira CAF, NB Gonçalves, RE Rosim, AM Fernandes (2009). Determination of aflatoxins in peanut products in the northeast region of São Paulo, Brazil. *Intl J Mol Sci* 10:174–183
- Olorunshola OE, ME Irhebhude, AE Ewwiekpaefe (2023). A Comparative study of YOLOv5 and YOLOv7 object detection algorithms. *J Comput Soc Inform* 2:1–12
- Osaili TM, WAMB Odeh, MAL Ayoubi, AASAA Ali, MSA Sallagi, RS Obaid, V Garimella, Bakhit, FSB Bakhit, R Holley, NEI Darra (2023). Occurrence of aflatoxins in nuts and peanut butter imported to UAE. *Heliyon* 9:e14530
- Phan QH, VT Nguyen, CH Lien, TP Duong, MTK Hou, NB Le (2023). Classification of tomato fruit using Yolov5 and convolutional neural network models. *Plants* 12:790
- Polisenska I (2011). Identification of *Fusarium* damaged wheat kernels using image analysis. *Acta Univ Agric Silvicult Mendelianae Brunensis* 59:125–130
- Rotich V, DF Al Riza, F Giametta, T Suzuki, Y Ogawa, N Kondo (2020). Thermal oxidation assessment of Italian extra virgin olive oil using an ultraviolet (UV) induced fluorescence imaging system. *Spectrochim Acta - Part A: Mol Biomol Spectrosc* 237:118373
- Rushing BR, MI Selim (2019). Aflatoxin B1: A review on metabolism, toxicity, occurrence in food, occupational exposure, and detoxification methods. *Food Chem Toxicol* 124:81–100
- Sanchez SA, HJ Romero, AD Morales (2020). A review: Comparison of performance metrics of pretrained models for object detection using the TensorFlow framework. *IOP Conf Ser: Mater Sci Eng* 844:012024
- Tallada JG, DT Wicklow, TC Pearson, PR Armstrong (2011). Detection of fungus-infected corn kernels using near-infrared reflectance spectroscopy and color imaging. *Trans ASABE* 54:1151–1158
- Thiruppathi S (2016). Near-infrared (NIR ) hyperspectral imaging: Theory and applications to detect fungal infection and mycotoxin contamination in food products. *J Grain Storage Res* 1:90–99
- Thuan D (2021). Evolution of Yolo Algorithm and Yolov5: The State-of-the-art object detection algorithm. *Bachelor's Thesis*. DIN16SP, Information Technology, Oulu University of Applied Sciences, Oulu, Finland
- Voorra V, S Bermúdez, C Larrea (2019). Global market report: Cocoa. Available at: [https://www.scirp.org/\(S\(czeh2tfqw2orz553k1w0r45\)\)/reference/referencespapers.aspx?referenceid=3019686](https://www.scirp.org/(S(czeh2tfqw2orz553k1w0r45))/reference/referencespapers.aspx?referenceid=3019686) (Accessed: 22 September 2023)
- Wang L, WQ Yan (2021). Tree Leaves Detection Based on Deep Learning BT. In: *Geometry and Vision*, pp:26–38. Nguyen V, WQ Yan, H Ho (Eds.). Springer International Publishing. New York, USA
- Wang L, Y Zhao, Z Xiong, S Wang, Y Li, Y Lan (2022). Fast and precise detection of litchi fruits for yield estimation based on the improved YOLOv5 model. *Front Plant Sci* 13:965425
- Wu F (2015). Global impacts of aflatoxin in maize: Trade and human health. *World Mycotoxin J* 8:137–142
- Wu Y, JH Cheng, DW Sun (2021). Blocking and degradation of aflatoxins by cold plasma treatments: Applications and mechanisms. *Trends Food Sci Technol* 109:647–661
- Yadav PK, JA Thomasson, SW Searcy, RG Hardin, U Braga-Neto, SC Popescu, DE Martin, R Rodriguez, K Meza, J Enciso, JS Diaz, T Wang (2022). Assessing the performance of YOLOv5 algorithm for detecting volunteer cotton plants in corn fields at three different growth stages. *Artif Intellig Agric* 6:292–303
- Ye Z, W Wang, X Wang, F Yang, F Peng, K Yan, H Kou, A Yuan (2023). Traffic flow and vehicle speed monitoring with the object detection method from the roadside distributed acoustic sensing array. *Front Earth Sci* 10:992571